

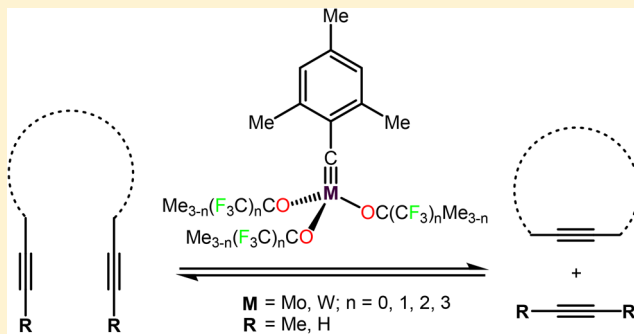
Tuning the Catalytic Alkyne Metathesis Activity of Molybdenum and Tungsten 2,4,6-Trimethylbenzylidyne Complexes with Fluoroalkoxide Ligands $\text{OC}(\text{CF}_3)_n\text{Me}_{3-n}$ ($n = 0-3$)

Celine Bittner,[†] Henrike Ehrhorn,[†] Dirk Bockfeld, Kai Brandhorst, and Matthias Tamm^{*†}

Institut für Anorganische und Analytische Chemie, Technische Universität Braunschweig, Hagenring 30, 38106 Braunschweig, Germany

Supporting Information

ABSTRACT: The molybdenum and tungsten 2,4,6-trimethylbenzylidyne complexes $[\text{MesC}\equiv\text{M}\{\text{OC}(\text{CF}_3)_n\text{Me}_{3-n}\}_3]$ ($\text{M} = \text{Mo}: \text{MoF}_0, n = 0; \text{MoF}_3, n = 1; \text{MoF}_6, n = 2; \text{MoF}_9, n = 3; \text{M} = \text{W}: \text{WF}_3, n = 1; \text{Mes} = 2,4,6\text{-trimethylphenyl}$) were prepared by the reaction of the tribromides $[\text{MesC}\equiv\text{MBr}_3(\text{dme})]$ ($\text{dme} = 1,2\text{-dimethoxyethane}$) with the corresponding potassium alkoxides $\text{KOC}(\text{CF}_3)_n\text{Me}_{3-n}$. The molecular structures of all complexes were established by X-ray diffraction analysis. The catalytic activity of the resulting alkylidyne complexes in the homometathesis and ring-closing alkyne metathesis of internal and terminal alkynes was studied, revealing a strong dependency on the fluorine content of the alkoxide ligand. The different catalytic performances were rationalized by DFT calculations involving the metathesis model reaction of 2-butyne. Because the calculations predict the stabilization of metallacyclobutadiene (MCBD) intermediates by increasing the degree of fluorination, **MoF9** was treated with 3-hexyne to afford the MCBD complex $[(\text{C}_3\text{Et}_3)\text{Mo}\{\text{OC}(\text{CF}_3)_3\}_3]$, which was characterized spectroscopically.



INTRODUCTION

The number of well-defined homogeneous alkyne metathesis catalysts that are capable of efficiently promoting the reversible cleavage and formation of carbon–carbon triple bonds has steadily grown over the past decade.^{1–7} Recent developments were commenced with imidazolin-2-iminato tungsten alkylidyne complexes of type I (Figure 1),^{8–15} which were developed drawing on the structure of the most active alkene metathesis catalysts, i.e., Schrock-type alkylidene complexes.^{2,16–18} Besides these asymmetrically substituted alkylidyne complexes, all other recent additions to the group of highly active alkyne metathesis catalysts feature a symmetric set of ancillary ligands X as in $[\text{RC}\equiv\text{MX}_3]$. Thereby, molybdenum alkylidyne complexes such as **II** with triphenylsiloxide ligands ($\text{X} = \text{OSiPh}_3$)^{19,20} represent the most frequently used catalysts in natural product synthesis, predominantly through ring-closing alkyne metathesis (RCAM).^{21–28} Siloxide ligands, namely $\text{X} = \text{OSi}(\text{OtBu})_3$, were also employed for the preparation of the tungsten alkylidyne complex **III**, which proved catalytically active not only in alkyne metathesis²⁹ but also in the metathesis of conjugated diynes.^{30,31} Molybdenum alkylidyne complexes such as **IV** supported by chelating phenoxide ligands represent another important class of well-defined catalysts^{32–35} that have found application in polymer synthesis^{36–39} and, most notably, in the construction of supramolecular aryleneethynylene macrocycles and cages through alkyne metathesis.^{40–46}

Since the early 1980s, fluorinated and nonfluorinated alkoxides (OR^F) of the type $\text{OCH}(\text{CF}_3)_2$ and $\text{OC}(\text{CF}_3)_n\text{Me}_{3-n}$ ($n = 0-3$) have been the most widely used ligand systems for the preparation of high oxidation state complexes with metal–carbon multiple bonds.^{17,47,48} Hence, neopentylidyne complexes $[\text{Me}_3\text{CC}\equiv\text{M}(\text{OR}^F)_3]$ ($\text{M} = \text{Mo}, \text{W}$), or solvated species such as $[\text{Me}_3\text{CC}\equiv\text{M}(\text{OR}^F)_3(\text{dme})]$ ($\text{dme} = 1,2\text{-dimethoxyethane}$), have been shown to be highly active, e.g., in the metathesis of 3-heptyne.^{49–52} These studies clearly revealed a strong dependency of the alkyne metathesis activity on the metal–ligand combination; for instance, comparison of the unfluorinated species $[\text{Me}_3\text{CC}\equiv\text{M}(\text{OCMe}_3)_3]$ indicated superior performance of the tungsten complex.^{49,52,53} The reverse order was found for the hexafluoro-*tert*-butoxide species $[\text{Me}_3\text{CC}\equiv\text{M}\{\text{OC}(\text{CF}_3)_2\text{Me}\}_3]$ with the Mo system representing one of the best alkyne metathesis catalysts studied by the Schrock group.^{50–52}

The closely related 2,4,6-trimethylbenzylidyne complex $[\text{MesC}\equiv\text{M}\{\text{OC}(\text{CF}_3)_2\text{Me}\}_3]$ (**MoF6**) was prepared via the so-called low-oxidation-state route from $\text{Mo}(\text{CO})_6$.¹¹ The steric demand of the Mes substituent allowed for easy removal of coordinating solvents (THF or DME), which was found to be beneficial for the catalytic performance.⁵⁴ In fact, **MoF6** exhibits unprecedented catalytic activity,⁵⁵ and it is even

Received: July 11, 2017

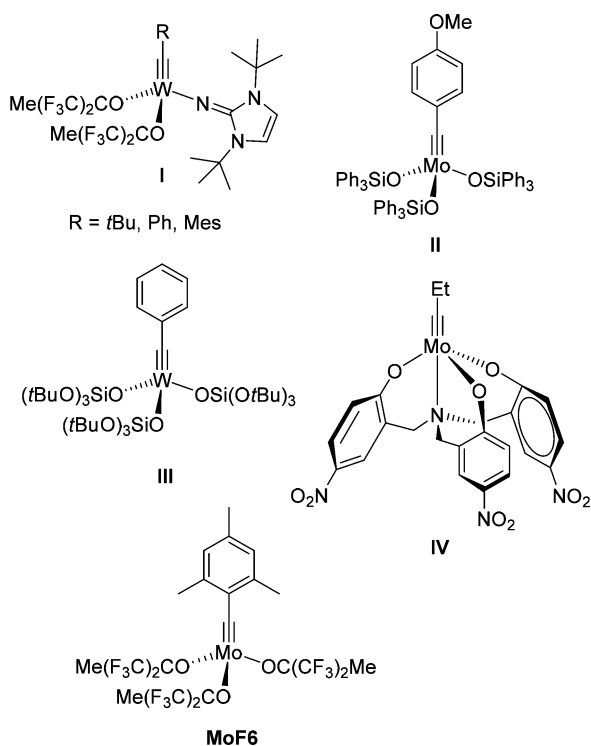


Figure 1. Well-defined catalysts for alkyne metathesis.

capable of efficiently metathesizing terminal alkynes,^{54–56} a reactivity that was recently also uncovered for **II**.^{23,57} It should be noted that previous attempts to promote terminal alkyne metathesis (TAM), e.g., with $[\text{Me}_3\text{CC}\equiv\text{W}(\text{OCMe}_3)_3]$, proved significantly less efficient,^{58–61} which was ascribed to deprotonation of intermediate metallacyclobutadiene species and formation of deprotonated metallacycles.^{52,62,63} The latter species are expected to be responsible for the observed high activity toward alkyne polymerization. Lately, **MoF6** and related species have also been successfully employed in ring-opening alkyne metathesis polymerization (ROAMP).^{64,65}

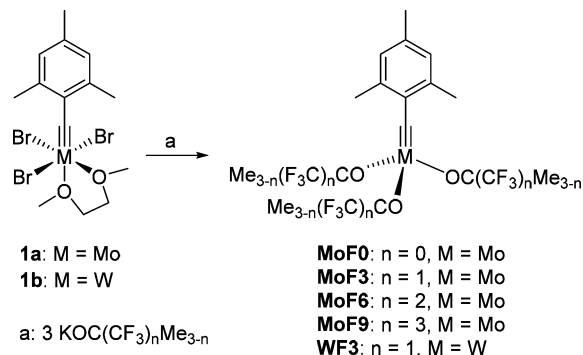
To affirm whether the optimum degree of fluorination in combination with the metal atom (Mo) has already been realized in **MoF6**, we wish to present herein the synthesis and structural characterization of the complete series of molybdenum complexes $[\text{MesC}\equiv\text{Mo}\{\text{OC}(\text{CF}_3)_n\text{Me}_{3-n}\}_3]$ (**MoF0**, $n = 0$; **MoF3**, $n = 1$; **MoF6**, $n = 2$; **MoF9**, $n = 3$) together with a combined experimental and theoretical study of their catalytic alkyne metathesis activity. From the corresponding series of tungsten complexes, $[\text{MesC}\equiv\text{W}\{\text{OC}(\text{CF}_3)_n\text{Me}_{3-n}\}_3]$, we aimed exclusively at the synthesis of **WF3** ($n = 1$) because **WF6** ($n = 2$) and **WF9** ($n = 3$) were already shown to be inactive in alkyne metathesis,^{13,54} which was attributed to the higher electrophilicity of tungsten alkylidyne complexes in comparison with their molybdenum relatives.⁴⁸ **WF0** ($n = 0$) was also not included in this study as its neopentylidene congener $[\text{Me}_3\text{CC}\equiv\text{W}(\text{OCMe}_3)_3]$ has been widely used in alkyne metathesis, albeit usually at elevated temperature and with higher catalyst loadings.^{1,49,53,58,59}

RESULTS AND DISCUSSION

Preparation and Characterization of 2,4,6-Trimethylbenzylidene Molybdenum and Tungsten Complexes. Following the low-oxidation-state route,¹¹ the 2,4,6-trimethylbenzylidene complexes of molybdenum and tungsten are easily

accessible from the tribromides $[\text{MesC}\equiv\text{MBr}_3(\text{dme})]$ (**1a**, $\text{M} = \text{Mo}$; **1b**, $\text{M} = \text{W}$) synthesized through a two-step protocol starting with molybdenum or tungsten hexacarbonyl and mesityllithium (MesLi).⁵⁴ Treatment of **1a** or **1b** with three equivalents of the potassium alkoxides $\text{KOC}(\text{CF}_3)_n\text{Me}_{3-n}$ ($n = 0–3$) resulted in the formation of the trisalkoxide complexes **MoF0–MoF9** and **WF3** (Scheme 1). As described for the

Scheme 1. Synthesis of 2,4,6-Trimethylbenzylidene Complexes



synthesis of **MoF6**,⁵⁴ the preparations of **MoF0** and **WF3** were accomplished by reaction of **1a** or **1b** with the respective alkoxides in THF. After stirring for 16 h, evaporation at slightly elevated temperature, extraction of the residual with pentane, and recrystallization at -40 °C afforded the products as yellow crystalline solids in 45 and 72% yields, respectively. When treating **1a** with three equivalents of the trifluoro-*tert*-butoxide $\text{KOC}(\text{CF}_3)_2\text{Me}$ in THF, significant amounts of the corresponding dimolybdenum hexaalkoxide were formed. This complex featuring a Mo–Mo triple bond has been reported previously;⁶⁶ details of its spectroscopic characterization and of an X-ray diffraction analysis can be found in Figure S23 and Table S3. The use of toluene as solvent and diethyl ether for recrystallization furnished sufficient amounts of **MoF3**, albeit in comparatively low yield (31%). Treatment of **1a** with the perfluoro-*tert*-butoxide $\text{KOC}(\text{CF}_3)_3$ in THF gave exclusively the solvate **MoF9**-thf with a strongly bound THF ligand; this complex had previously proved inactive in catalytic alkyne metathesis.¹³ Performing the same reaction in toluene solution with longer reaction times (3 d) afforded the desired THF-free product in 45% yield as a red crystalline solid.

In the ^{13}C NMR spectra, the carbyne carbon atoms generate characteristic lowfield signals. As anticipated, the chemical shift of the alkylidyne carbon atom increases with the degree of alkoxide fluorination. Thus, the alkylidyne resonance of nonfluorinated **MoF0** can be found at 296.9 ppm, whereas the resonances of the fluorinated alkylidynes **MoF3**, **MoF6**, and **MoF9** appear at gradually lower fields at 307.1, 317.6, and 332.7 ppm, respectively. These values fall in the range typically observed for molybdenum alkylidyne complexes.^{13,52} The ^{13}C NMR signal for the carbyne carbon atom of **WF3** is found slightly more upfield at 282.3 ppm in comparison to the molybdenum species, which can be ascribed to the higher electrophilicity of the tungsten metal.^{50,54} This signal shows the expected satellites owing to coupling with the ^{183}W isotope, i.e., $^1J_{\text{CW}} = 147$ Hz. The ^{19}F NMR spectra of the fluorinated complexes show only one singlet each at -82.7 , -78.1 , and -73.1 ppm for **MoF3**, **MoF6**, and **MoF9** and at -82.7 ppm for

WF3, which indicates fast rotation of the mesityl group at room temperature on the NMR time scale.

The molecular structures of all complexes were established by X-ray diffraction analysis; ORTEP diagrams of MoF3 and WF3 are shown in Figure 2, and the molecular structures of

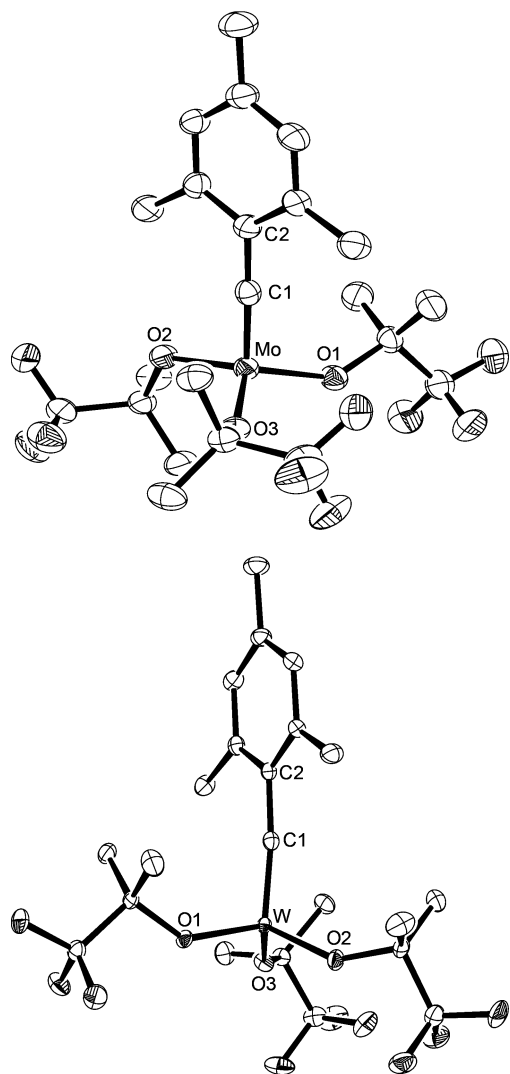


Figure 2. ORTEP diagram of MoF3 (top) and WF3 (bottom) with thermal displacement parameters drawn at 50% probability; hydrogen atoms are omitted for clarity.

MoF0 and MoF9 can be found in Figure S22. Pertinent structural data are assembled in Table 1. All complexes show distorted tetrahedral geometries around the metal atom. As observed for MoF6,⁵⁴ the complexes adopt approximate C_s symmetry with the mesityl group in a coplanar alignment with

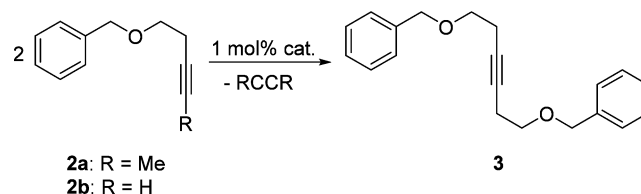
Table 1. Selected Bond Lengths, Angles, and ^{13}C NMR Shifts of Complexes MoF0–MoF9 and WF3

	M–C1 [Å]	M–C1–C2 [deg]	δ [ppm]
MoF0	1.747(3)	176.3(2)	296.9
MoF3	1.747(2)	175.28(18)	307.1
MoF6	1.74738(16)	177.40(16)	317.6
MoF9	1.74729(16)	173.86(13)	332.7
WF3	1.7689(19)	173.64(14)	282.3

the pseudomirror plane. In contrast, a perpendicular orientation of the mesityl group is observed for WF3. Short metal–carbon bonds together with almost linear M–C1–C2 axes are found for all complexes. Within experimental error, the Mo–C1 distances of ~ 1.75 Å are identical in MoF0, MoF3, MoF6, and MoF9, revealing a negligible impact of the degree of fluorination. As observed for other Mo/W pairs,^{11,13,54} the W–C1 bond in WF3 of 1.7689(19) Å is slightly longer compared to MoF3 and the other molybdenum complexes. The M–C1–C2 angles range from $173.64(14)^\circ$ in WF3 to $177.40(16)^\circ$ in MoF6 (Table 1).

Catalytic Alkyne Metathesis with 2,4,6-Trimethylbenzylidene Molybdenum and Tungsten Complexes. To examine the catalytic potential of the alkyldiyne complexes and to compare their performance with theoretically predicted activities (vide infra), we investigated the homometathesis of various internal and terminal alkynes. Initially, 3-pentynyl benzyl ether (2a) and 3-butynyl benzyl ether (2b) were used as well-established test substrates (Scheme 2).^{54,55} Toluene

Scheme 2. Homometathesis of the Benzyl Ethers 2a and 2b



solutions of the substrates with catalyst loadings of 1 mol % were stirred at room temperature in the presence of molecular sieves (5 Å MS) as 2-butyne or acetylene scavenger. The reactions were monitored by gas chromatography with *n*-decane as internal standard, and the resulting conversion versus time diagrams are shown in Figures 3 and 4. Figure 3 reveals

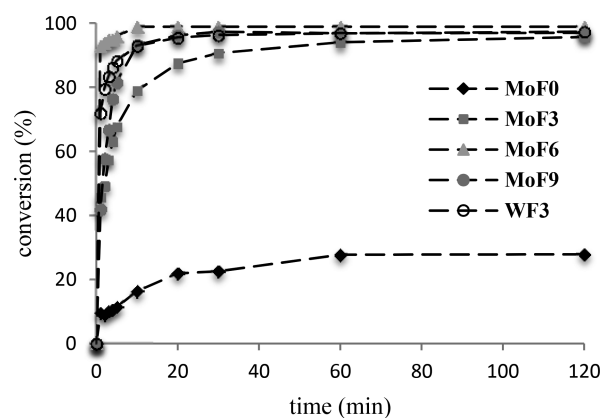


Figure 3. Conversion versus time diagram for the metathesis of 3-pentynyl benzyl ether (2a, 0.5 mmol) in toluene (2.5 mL) catalyzed by 1 mol % of MoF0–MoF9 and WF3 in the presence of 5 Å MS at room temperature.

that all catalysts are active in the metathesis of 2a at room temperature. Even the least active system MoF0 achieves a moderate conversion of 35% after 2 h. All other catalysts, MoF3, MoF6, MoF9, and WF3, accomplish almost full conversion within 120 min with MoF6 showing the highest activity. For better comparison of the initial rates, plots of conversion against a logarithmic timeline can be found in

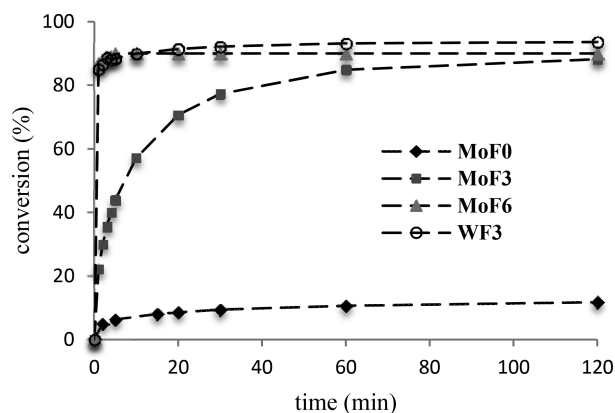


Figure 4. Conversion versus time diagram for the metathesis of 3-butynyl benzyl ether (**2b**, 0.5 mmol) in toluene (24 mL) catalyzed by 1 mol % of **MoF0**–**MoF6** and **WF3** in the presence of 5 Å MS at room temperature; **MoF9** gave around 10% conversion with exclusive formation of polymeric material.

Figure S1. Metathesis product **3** could be isolated in good yields by filtration through alumina and evaporation of the solvent. **MoF6** provides the highest isolated yield of 96%, whereas **MoF3**, **MoF9**, and **WF3** afforded yields of 94, 89, and 93%, respectively (**Table 2**).

Similar results were obtained using the corresponding terminal alkyne **2b** at significantly lower substrate concentration to avoid side reactions such as polymerization (**Figure 4**). Under these conditions, **MoF9** proved completely inactive in terminal alkyne metathesis (TAM), and polymeric material was isolated instead and analyzed by gel permeation chromatography ($M_n = 802.1 \text{ g mol}^{-1}$, $M_w = 1803.3 \text{ g mol}^{-1}$). Low conversion of only 12% was found for **MoF0** after 2 h. In the same period, 88% conversion and 84% isolated yield were obtained with **MoF3**. Surprisingly, **MoF6** and **WF3** proved to be almost equally active, and very fast initiation rates $>80 \text{ min}^{-1}$ were observed for both catalysts (see **Figure S2**). From these reactions, **3** was isolated in 90 and 94% yields, respectively (**Table 2**). It should be emphasized that **WF3** represents the first tungsten alkylidyne complex that is able to promote the metathesis of terminal alkynes in an efficient manner.^{58–62}

Table 2. Alkyne Metathesis of Internal and Terminal Alkynes^a

Substrate	Product		Yield [%]				
			MoF0	MoF3	MoF6 ⁵⁴	MoF9	WF3
 2a , R=Me 2b , R=H	 3	R = Me	28 ^b	94	98	89	93
		R = H	12 ^b	84	90	- ^c	94
 4a , R=Me 4b , R=H	 5	R = Me	35 ^b	93	95	92	77
		R = H	8 ^b	53	92	- ^c	90
 6a , R=Me 6b , R=H	 7	R = Me	43 ^b	91	98	80	96
		R = H	13 ^b	85	96	- ^c	92
 8a , R=Me 8b , R=H	 9	R = Me	45 ^b	92	99	76	91
		R = H	11 ^b	90	95	- ^c	- ^d
 2b + SiMe ₃	 10		-	32 ^b	98	- ^c	95

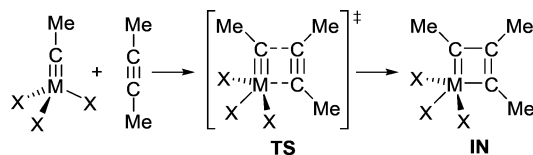
^aHomometathesis: substrate (0.5 mmol), catalyst (1 mol %), toluene (internal alkynes: 2.5 mL, 200 mM; terminal alkynes: 24 mL, 21 mM), 5 Å MS (500 mg), 25 °C, 2 h. RCAM: substrate (0.5 mmol), catalyst (2 mol %), toluene (internal alkynes: 24 mL, 21 mM; terminal alkynes: 112 mL, 4.5 mM), 5 Å MS (1 g), 25 °C, 2 h. ACM: substrates (0.25 mmol each), catalyst (1 mol %), toluene (12 mL, 21 mM), 5 Å MS (250 mg), 25 °C, 2 h. ^bGC yield after 2 h; all other yields are averaged isolated yields based on at least two runs. ^cNo yield obtained due to polymerization of the substrate. ^dUnexpectedly, several runs with different substrate and catalyst samples did not result in any conversion.

Encouraged by these results, we further studied the substrate scope for all catalysts (Table 2). Thus, we attempted homometathesis of benzoic esters **4** and RCAM of α,ω -diynes **6** and **8** bearing either 3-pentynyl (**a**: R = Me) or 3-butynyl (**b**: R = H) groups. For the benzoic esters **4**, the metathesis reaction was performed analogously to the benzyl ethers **2**, whereas the RCAM reactions with **6** and **8** were performed at lower substrate concentration of 21 mM for internal and 4.5 mM for terminal substrates with catalyst loadings of 2 mol % in the presence of molecular sieves (5 Å). In principle, the results resemble the situation established with substrates **2**; MoF6 and WF3 show the best performance with high isolated yields of almost all products. For unknown reasons, however, RCAM of **8b** with WF3 repeatedly gave no conversion at all. MoF3 also afforded good yields despite its overall lower activity. As observed for substrates **2**, MoF9 can only accomplish the metathesis of internal alkynes in a satisfactory manner but fails completely in the metathesis of all terminal alkynes. MoF0 as the least active catalyst gave only moderate or low conversions as indicated by GC analysis.

The best catalysts MoF3, MoF6, and WF3 were also employed for the alkyne cross metathesis (ACM) of the terminal benzyl ether **2b** with trimethylsilylacetylene. Mixtures of both substrates (1:1, 0.25 mmol each) were stirred in toluene for 2 h at room temperature with catalyst loadings of 1 mol %. Workup afforded unsymmetrical alkyne **10** in excellent yields in the cases of MoF6 (98%)⁵⁵ and WF3 (95%), whereas only 32% GC conversion into **10** was observed for MoF3 after 2 h. At this point, homometathesis product **3** was present in 58%. After 24 h, however, GC analysis indicated 75 and 17% conversion into products **10** and **3**, respectively. For conversion versus time diagrams, see Figures S3–S5. To the best of our knowledge, MoF6 and WF3 represent the first catalysts that can promote ACM of two terminal alkynes efficiently, whereas several ACM reactions involving one terminal and one internal alkyne, e.g., 1-trimethylsilylpropyne, were reported with **II**.⁵⁷ We assume that this process is driven thermodynamically with silylated product **10** being (slightly) more stable than homocoupled alkynes **3** and bis(trimethylsilyl)acetylene.

Theoretical Investigation of Alkyne Metathesis with Molybdenum and Tungsten Alkylidyne Complexes. To explain the different activities of the Mo and W alkylidyne complexes depending on the degree of alkoxide fluorination, we performed a series of theoretical calculations using the B3LYP density functional.^{67,68} For this purpose, the metathesis of 2-butyne was selected as a model reaction (Scheme 3), which had

Scheme 3. Model Reaction of 2-Butyne with Trialkoxide Ethylidyne Complexes (M = Mo, W; X = OMe₃, OC(CF₃)Me₂, OC(CF₃)₂Me, OC(CF₃)₃)



previously been used to rationalize the relative activities of Mo and W alkyne metathesis catalysts in a reliable fashion.^{10,11,69} For the model alkylidynes [MeC≡MX₃] (M = Mo, W; X = OMe₃, OC(CF₃)Me₂, OC(CF₃)₂Me, OC(CF₃)₃), the first three relevant stationary points of the rate-determining step (catalyst plus 2-butyne, transition state TS, metallacyclobuta-

diene intermediate IN) were computed. Enthalpic and entropic contributions were calculated by statistical thermodynamics as implemented in the Gaussian09 set of programs.⁷⁰ A full catalytic cycle additionally includes the interconversion between two metallacyclobutadiene (MCBD) intermediates. However, this rearrangement has a considerably lower barrier,⁸ and therefore, no attempts were made to locate this second transition state. Furthermore, it should be mentioned that entropic effects for the associative mechanism at work are expected to be smaller in the condensed phase, which should lead to significantly lower free activation barriers in comparison with these gas-phase computations.⁷¹ The following discussion will therefore be based on the calculated enthalpies, which are listed in Tables 3 and 4 along with additional thermodynamic data.

Table 3. Relative B3LYP Energies and Enthalpies (kcal mol⁻¹) for the Model Metathesis Reaction of 2-Butyne with MoF0–MoF9^a

	TS ^b			IN ^b		
	ΔE_0^\ddagger	ΔH_{298}^\ddagger	ΔG_{298}^\ddagger	ΔE_0	ΔH_{298}	ΔG_{298}
MoF0	23.28	22.47	38.82	16.19	15.39	30.89
MoF3	18.57	17.72	34.93	12.68	11.83	28.39
MoF6	7.18	6.29	24.44	1.42	0.57	18.00
MoF9	5.14	4.28	21.93	-2.19	-3.26	15.38

^aFor more details, see Supporting Information. ^b ΔE_0 : relative energies at 0 K, ΔH_{298} : enthalpies at 298 K, ΔG_{298} : Gibbs free energies at 298 K; all values are stated relative to the isolated catalyst and 2-butyne.

Table 4. Relative B3LYP Energies and Enthalpies (kcal mol⁻¹) for the Model Metathesis Reaction of 2-Butyne with WF0–WF9^a

	TS ^b			IN ^b		
	ΔE_0^\ddagger	ΔH_{298}^\ddagger	ΔG_{298}^\ddagger	ΔE_0	ΔH_{298}	ΔG_{298}
WF0	17.26	16.63	32.92	6.31	5.51	21.00
WF3	16.58	16.03	32.70	2.55	1.68	18.31
WF6	10.04	9.65	26.24	-7.70	-8.82	10.76
WF9	9.43	9.02	25.41	-11.32	-12.29	6.26

^aFor more details, see Supporting Information. ^b ΔE_0 : relative energies at 0 K, ΔH_{298} : enthalpies at 298 K, ΔG_{298} : Gibbs free energies at 298 K; all values are stated relative to the isolated catalyst and 2-butyne.

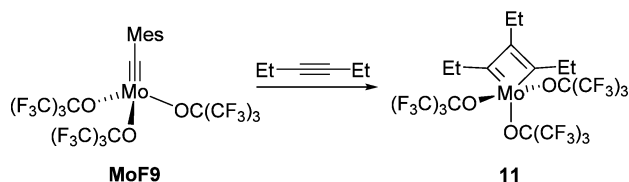
The calculations predict an increasing relative stability of the metallacyclobutadienes (IN) for both sets of molybdenum and tungsten complexes with an increasing degree of fluorination on the alkoxide ligands. For the same degree of fluorination, the tungsten metallacyclobutadienes are significantly more stabilized (by at least 9 kcal mol⁻¹) compared to their molybdenum congeners, which can be ascribed to the greater electrophilic character of tungsten alkoxides.⁴⁸ A similar trend can be observed for the transition states, suggesting that the formation of the metallacyclobutadienes is not only favored thermodynamically but also kinetically with increasing the degree of fluorination. Because these metallacyclobutadienes are crucial intermediates in alkyne metathesis (Scheme 3),^{72–75} it is expected that the catalytic activity increases in the same order. A full catalytic cycle, however, also involves a [2 + 2] cycloreversion, which could also become the rate-determining step if the metallacyclobutadiene is more stable than the respective alkylidyne complex and alkyne. This is most likely

the case for the intermediates derived from **MoF9**, **WF6**, and **WF9** for which our computations predict negative enthalpies.

In agreement with the experimental findings, the increase in catalytic activity in the order **MoF0** < **MoF3** < **MoF6** correlates with the decreasing activation barrier, whereas the lower catalytic activity of **MoF9** compared to that of **MoF6** can be ascribed to an overly stabilized MCBD intermediate. Alkylidyne complexes of the type **WF0**, e.g., $\text{Me}_3\text{CC}\equiv\text{W}(\text{OCMe}_3)_3$, have been studied intensely by R. R. Schrock and A. Fürstner and showed good catalytic activity in homometathesis and RCAM reactions, usually at elevated temperature.^{17,50,76–79} Although we did not directly compare **WF0** and **WF3**, the catalytic performance of **WF3** appears to be superior, and unlike the **WF0** derivative $\text{Me}_3\text{CC}\equiv\text{W}(\text{OCMe}_3)_3$,^{58–60} it can even transform terminal alkynes efficiently at room temperature. Further increasing the degree of fluorination is counterproductive, and as previously reported, **WF6** and **WF9** show no catalytic activity in alkyne metathesis.^{54,13} This observation can again be ascribed to a significantly exothermic MCBD formation.

Formation of an Isolable Molybdenacyclobutadiene by Stoichiometric Reactions. Because the calculated enthalpies suggest a potentially stable MCBD derived from **MoF9**, we attempted to isolate such an intermediate. Therefore, a saturated CH_2Cl_2 solution of **MoF9** was treated with ten equivalents of 3-hexyne, which resulted in an immediate color change from red to purple, and upon refrigeration at 3 °C, a purple crystalline product formed. The crystals were suitable for X-ray diffraction analysis; however, the structure could not be refined because of severe disorder. An ORTEP plot revealing the connectivity and further information can be found in Figure S24 and Table S3. NMR analysis of the crystalline product in CD_2Cl_2 solution revealed the formation of metallacyclobutadiene **11**. The ^1H NMR spectrum shows signals corresponding to two different ethyl groups in a 2:1 ratio. The ^{13}C NMR spectrum also shows the lowfield chemical shifts expected for molybdenacycles at 269.9 ppm for the α carbon atoms and at 156.0 ppm for the β carbon atom, which is in good agreement with the NMR data reported for other molybdenacyclobutadienes.^{51,52,80} The ^{19}F NMR spectrum exhibits two multiplets at -72.6 (18F) and -72.7 ppm (9F), indicating the presence of two sets of alkoxide ligands. The formation of **11** can be explained by conversion of the 2,4,6-trimethylbenzylidyne ($\text{MesC}\equiv\text{Mo}$) into a propylidyne moiety ($\text{EtC}\equiv\text{Mo}$) and subsequent cycloaddition of a second equivalent of 3-hexyne (Scheme 4).

Scheme 4. Preparation of Metallacyclobutadiene 11 with MoF9



It should be noted that **11** represents a rare example of an isolable molybdenacyclobutadiene,^{51,52,80} whereas significantly more tungstenacyclobutadienes of the type $[(\text{C}_3\text{R}_3)\text{WX}_3]$ (R = alkyl, aryl; X = alkoxide, phenoxide, amide, halide) have been reported.^{50,81–83} Paramagnetic MCBD-type complexes were recently isolated from the reaction of **MoF6** with diaminoace-

tylenes and structurally characterized, but theoretical calculations revealed that these systems are best described as Mo(IV) species containing anionic diaminodicarbene ligands of the type $[(\text{R}_2\text{N})\text{CC}(\text{Mes})\text{C}(\text{NR}_2)]^-$.⁸⁴

CONCLUSIONS

Comparison of the series of molybdenum alkylidyne complexes $[\text{MesC}\equiv\text{Mo}\{\text{OC}(\text{CF}_3)_n\text{Me}_{3-n}\}_3]$ ($n = 0–3$) with varying fluorine content reveals that **MoF6** ($n = 2$) shows the overall best catalytic performance in the metathesis of internal and terminal alkynes. Lower or higher fluorine content diminishes the catalytic activity, and **MoF0** ($n = 0$), **MoF3** ($n = 1$), and **MoF9** ($n = 3$) clearly exhibit inferior performance. This trend can be rationalized by DFT calculations on the metathesis model reaction of 2-butyne, which predict higher activation barriers for the formation of the metallacyclobutadiene (MCBD) intermediate for **MoF0** and **MoF3**, whereas the lower catalytic activity of **MoF9** can be ascribed to an overly stabilized MCBD. This conclusion is supported by isolation of the stable MCBD complex **11** by reaction of **MoF9** with 3-hexyne. These results indicate that the optimum level of fluorination for the application of molybdenum alkylidynes in alkyne metathesis catalysts is realized in **MoF6**.

Owing to the higher electrophilicity of their tungsten alkylidyne congeners $[\text{MesC}\equiv\text{W}\{\text{OC}(\text{CF}_3)_n\text{Me}_{3-n}\}_3]$, the calculations predict significantly stabilized MCBD intermediates for **WF6** and **WF9** in agreement with their catalytic inefficiency. Therefore, the optimum degree of fluorination in this series of tungsten-based alkyne metathesis catalysts is already attained in **WF3**, which showed excellent catalytic performance in the metathesis of internal and even terminal alkynes. These results confirm that the development of efficient alkyne metathesis catalysts based on molybdenum and tungsten alkylidyne complexes requires an elaborate adjustment of the metal/ligand combination, which considers that more electron-withdrawing, or more electronegative, ligands are needed for the Mo systems than for the more electrophilic W systems.

EXPERIMENTAL SECTION

General Experimental Considerations. All operations with air- and moisture-sensitive compounds were conducted in a glovebox (MBraun 200B) under a dry and oxygen-free argon atmosphere or on a Schlenk line using standard Schlenk techniques. Solvents were purified and dried by a Braun Solvent Purification System and stored over a molecular sieve (3–4 Å). Complexes **1a**, **1b**, and **MoF6**, the substrates **2**, **4**, **6**, and **8**,^{11,54,9} and the alkoxides (except for KOCMe_3) were synthesized according to literature methods. All other compounds were obtained from commercial sources and used without further purification. The molecular sieve 5 Å MS (Sigma-Aldrich, powder <50 μm) for metathesis reactions was dried for 24 h at 180 °C under vacuum prior to use. Sodium and potassium hydride dispersions in mineral oil were washed several times with hexane and dried under vacuum directly before use.

Analytical Methods. ^1H , ^{19}F , and ^{13}C NMR spectra were recorded on Bruker AV II-300, DRX-400, and AV II-600 instruments at room temperature. Chemical shifts (δ) are expressed in ppm (parts per million). ^1H and ^{13}C NMR spectra are referenced to residual solvent signals (C_6D_6 : $\delta(\text{H})$ 7.16 ppm, $\delta(\text{C})$ 128.06 ppm; CDCl_3 : $\delta(\text{H})$ 7.26 ppm, $\delta(\text{C})$ 77.16 ppm; CD_2Cl_2 : $\delta(\text{H})$ 5.32 ppm, $\delta(\text{C})$ 53.84 ppm). For ^{19}F NMR, an external calibration with CFCl_3 was used. Coupling constants (J) are reported in hertz (Hz). Multiplicities are expressed with s (singlet), d (doublet), t (triplet), q (quartet), or m (multiplet). The number of hydrogen atoms (n) for a signal is indicated by nH. When necessary, signal assignment was confirmed by two-dimensional ^1H , ^{13}C -HSQC NMR and ^1H , ^{13}C -HMBC NMR experi-

ments. Elemental analyses were accomplished by combustion and gas chromatographic analysis using a VarioMICRO Tube and WLD detection. Gas chromatography (GC) was executed on a Hewlett-Packard 5890 SERIES II using a DB5-HT column and FID detection. For calibration, *n*-decane was used as an internal standard. Gel permeation chromatography (GPC) was conducted on an Agilent Series 1200 instrument, which consisted of a PSS SDV (Lux) column (5 μ m, 100 Å \times 1000 Å). The flow-rate (THF) was maintained at 1 mL/min with the column temperature at 35 °C and elution monitored by an evaporative light-scattering detector.

Synthesis of MoF0. Compound **1a** (400 mg, 0.72 mmol) was added in small portions to a solution of KOCMe₃ (242 mg, 2.15 mmol) in THF (8 mL). The reaction mixture was stirred for 16 h at ambient temperature. After removal of the solvent at 50 °C under reduced pressure, the residue was extracted with small amounts of pentane. The combined extracts were filtered through a short pad of Celite, and the filtrate was concentrated and stored at -40 °C, affording the product as light yellow crystals. Yield: 144 mg (45%). ¹H NMR (600.1 MHz, C₆D₆, 298 K): δ 6.69 (m, 2H, *m*-CH), 2.85 (s, 6H, *o*-CH₃), 2.10 (s, 3H, *p*-CH₃), 1.46 (s, 27H, OC(CH₃)₃). ¹³C{¹H} NMR (150.9 MHz, C₆D₆, 298 K): δ 297.4 (s, Mo \equiv C), 143.5 (s, *i*-C), 139.3 (s, *o*-C), 136.5 (s, *p*-C), 128.2 (s, *m*-CH), 78.6 (s, OC(CH₃)₃), 32.3 (s, OC(CH₃)₃), 21.4 (s, *o*-CH₃), 21.1 (s, *p*-CH₃). Anal. Calcd for C₂₂H₃₈MoO₃: C 59.18, H 8.58. Found: C 58.98, H 8.34.

Synthesis of MoF3. Compound **1a** (200 mg, 0.36 mmol) was added in small portions to a solution of KOC(CF₃)Me₂ (179 mg, 1.08 mmol) in toluene (4 mL). The reaction mixture was stirred for 16 h at ambient temperature. After removal of the solvent under reduced pressure, the residue was extracted with small amounts of pentane and Et₂O. The combined extracts were filtered over a short pad of Celite, and the filtrate was dried under reduced pressure. Crystallization from Et₂O at -40 °C afforded the product in sufficient purity as yellow crystals. Yield: 68 mg (31%). ¹H NMR (600.1 MHz, C₆D₆, 298 K): δ 6.57 (m, 2H, *m*-CH), 2.64 (s, 6H, *o*-CH₃), 2.03 (s, 3H, *p*-CH₃), 1.44 (s, 18H, OC(CH₃)₂(CF₃)). ¹³C{¹H} NMR (150.9 MHz, C₆D₆, 298 K): δ 307.1 (s, Mo \equiv C), 143.1 (s, *i*-C), 140.2 (s, *o*-C), 138.9 (s, *p*-C), 128.2 (s, *m*-CH), 126.9 (q, ¹J_{CF} = 284 Hz, OC(CH₃)₂(CF₃)), 81.3 (q, ²J_{CF} = 29 Hz, OC(CH₃)₂(CF₃)), 24.5 (s, OC(CH₃)₂(CF₃)), 21.1 (s, *p*-CH₃), 20.8 (s, *o*-CH₃). ¹⁹F{¹H} NMR (282.5 MHz, C₆D₆, 298 K): δ -82.7 (s, CF₃). Anal. Calcd for C₂₂H₂₉F₉MoO₃: C 43.43, H 4.80. Found: C 43.26, H 4.75.

Synthesis of MoF9. A suspension of KOC(CF₃)₃ (1.0 g, 3.78 mmol) in toluene (10 mL) was added to **1a** (700 mg, 1.26 mmol) in toluene (10 mL). The reaction mixture was stirred for 3 days at ambient temperature. After removal of the solvent under reduced pressure, the red residue was extracted with small amounts of pentane. The combined extracts were filtered over a short pad of Celite, and the filtrate was concentrated and stored at -40 °C, affording the product as red crystals. To achieve purity suitable for catalysis, the product was recrystallized three times. Yield: 618 mg (53%). ¹H NMR (600.1 MHz, CD₂Cl₂, 298 K): δ 6.78 (m, 2H, *m*-CH), 2.50 (s, 6H, *o*-CH₃), 2.33 (s, 3H, *p*-CH₃). ¹³C{¹H} NMR (150.9 MHz, CD₂Cl₂, 298 K): δ 332.7 (s, Mo \equiv C), 143.7 (s, *o*-C), 143.3 (s, *i*-C), 143.2 (s, *p*-C), 128.9 (s, *m*-CH), 120.7 (q, ¹J_{CF} = 293 Hz, OC(CF₃)₃), 85.5 (m, ²J_{CF} = 31 Hz, OC(CF₃)₃), 21.3 (s, *p*-CH₃), 19.7 (s, *o*-CH₃). ¹⁹F{¹H} NMR (376.1 MHz, CD₂Cl₂, 298 K): δ -73.69 (s, CF₃). Anal. Calcd for C₂₂H₁₁F₂₇MoO₃: C 28.34, H 1.19. Found: C 28.44, H 1.56.

Synthesis of WF3. Compound **1b** (200 mg, 0.31 mmol) was added in small portions to a solution of KOC(CF₃)Me₂ (155 mg, 0.93 mmol) in THF (4 mL). The reaction mixture was stirred for 16 h at ambient temperature. After removal of the solvent under reduced pressure at 50 °C, the residue was extracted with small amounts of pentane. The combined extracts were filtered over a short pad of Celite, and the filtrate was concentrated and stored at -40 °C affording the product as yellow crystals. Yield: 156 mg (72%). ¹H NMR (600.1 MHz, C₆D₆, 298 K): δ 6.78 (m, 2H, *m*-CH), 2.74 (s, 6H, *o*-CH₃), 2.23 (s, 3H, *p*-CH₃), 1.41 (s, 18H, OC(CH₃)₂(CF₃)). ¹³C{¹H} NMR (150.9 MHz, C₆D₆, 298 K): δ 282.3 (t, ¹J_{CW} = 147 Hz, W \equiv C), 141.3 (s, *i*-C), 141.0 (s, *o*-C), 137.3 (s, *p*-C), 127.3 (s, *m*-CH), 126.7 (q, ¹J_{CF} = 284 Hz, OC(CH₃)₂(CF₃)), 81.2 (q, ²J_{CF} = 29 Hz,

OC(CH₃)₂(CF₃)), 23.9 (s, OC(CH₃)₂(CF₃)), 20.4 (s, *p*-CH₃), 20.3 (s, *o*-CH₃). ¹⁹F{¹H} NMR (282.5 MHz, C₆D₆, 298 K): δ -82.8 (s, CF₃). Anal. Calcd for C₂₂H₂₉F₉WO₃: C 37.95, H 4.20. Found: C 37.87, H 4.23.

Synthesis of [(C₃Et₃)Mo(OC(CF₃)₃)₃]11**.** Ten equiv of 3-hexyne (88 mg, 1.07 mmol) was added to a solution of MoF9 (100 mg, 0.11 mmol) in CH₂Cl₂. The color of the reaction mixture immediately changed from red to purple. After cooling the solution to 3 °C for 2 days, purple crystals were obtained. Yield: 53 mg (55%). ¹H NMR (600.1 MHz, CD₂Cl₂, 298 K): δ 4.01 (q, 2H, ³J_{HH} = 7.6 Hz, C_βCH₂), 3.75 (q, 4H, ³J_{HH} = 7.3 Hz, C_αCH₂), 1.86 (t, 6H, ³J_{HH} = 7.3 Hz, C_βCH₂CH₃), 1.71 (t, 3H, ³J_{HH} = 7.6 Hz, C_αCH₂CH₃). ¹³C{¹H} NMR (150.9 MHz, CD₂Cl₂, 298 K): δ 269.9 (s, C_α), 156.0 (s, C_β), 121.3 (q, ¹J_{CF} = 295 Hz, equatorial-OC(CF₃)₃), 120.8 (q, ¹J_{CF} = 290 Hz, axial-OC(CF₃)₃), 83.1 (m, ²J_{CF} = 29 Hz, OC(CF₃)₃), 34.7 (s, C_αCH₂), 32.3 (s, C_βCH₂), 12.7 (s, C_βCH₂CH₃), 12.6 (s, C_αCH₂CH₃). ¹⁹F{¹H} NMR (376.1 MHz, CD₂Cl₂, 298 K): δ -72.6 (m, 18F, ⁴J_{FF} = 2.8 Hz, CF₃), -72.7 (m, 9F, ⁴J_{FF} = 2.8 Hz, CF₃). Anal. Calcd for C₂₁H₁₅F₂₇MoO₃: C 27.29, H 1.64; Found: C 27.24, H 1.26.

Comparison of Catalytic Activities. A 25 mL Schlenk flask under an Ar atmosphere was charged with 5 Å MS (250 mg), 0.05 mL of *n*-decane, and a solution of the substrate (0.25 mmol) in toluene (internal alkynes: 1.25 mL, terminal alkynes: 12 mL). Then, the catalyst (1 mol %) was added, and samples (internal alkynes: 0.05 mL, terminal alkynes: 0.25 mL) were taken for gas chromatographic analysis in certain intervals.

General Procedure for Homometathesis. A 50 mL Schlenk flask under an Ar atmosphere was charged with 5 Å MS (500 mg) and a solution of the substrate (0.5 mmol) in toluene (internal alkynes: 2.5 mL, terminal alkynes: 24 mL). Then, the catalyst (1 mol %) was added, and the mixture was stirred for 2 h at room temperature. The catalyst and the molecular sieve were removed by filtration through alumina, and the solvent was evaporated. The crude reaction product was purified by flash chromatography on silica gel with 1:8 ethyl acetate/hexane.

General Procedure for RCAM. A Schlenk flask under an Ar atmosphere was charged with 5 Å MS (1 g) and a solution of the substrate (0.5 mmol) in toluene (internal alkynes: 24 mL, terminal alkynes: 112 mL). Then, the catalyst (2 mol %) was added, and the mixture was stirred for 2 h at room temperature. The catalyst and the molecular sieve were removed by filtration through alumina, and the solvent was evaporated. The crude reaction product was purified by flash chromatography on silica gel with 1:8 ethyl acetate/hexane.

General Procedure for ACM. A 50 mL Schlenk flask under an Ar atmosphere was charged with 5 Å MS (250 mg) and a solution of the substrate (0.25 mmol) and trimethylsilyl-acetylene (0.25 mmol) in 12 mL of toluene. Then, the catalyst (1 mol %) was added, and the mixture was stirred for 2 h at room temperature. The catalyst and the molecular sieve were removed by filtration through alumina, and the solvent was evaporated. The crude reaction product was purified by flash chromatography on silica gel with 1:8 ethyl acetate/hexane.

■ ASSOCIATED CONTENT

Supporting Information

The Supporting Information is available free of charge via the Internet at . The Supporting Information is available free of charge on the ACS Publications website at DOI: 10.1021/acs.organomet.7b00519.

Spectroscopic characterization of all new compounds, details of the X-ray measurements of complexes MoF0 (CCDC 1560020), MoF3 (CCDC 1560021), MoF9 (CCDC 1560022), WF3 (CCDC 1560023), Mo₂{OC(CF₃)₂Me}₆ (CCDC 1560024), and **11** (CCDC 1566270) (PDF)

Optimized geometries of the molybdenum (MoF0–MoF9) and tungsten (WF0–WF9) complexes and their

corresponding transition states and intermediates during the alkyne metathesis with 2-butyne (MOL)

Accession Codes

CCDC 1560020–1560024 and 1566270 contain the supplementary crystallographic data for this paper. These data can be obtained free of charge via www.ccdc.cam.ac.uk/data_request/cif, or by emailing data_request@ccdc.cam.ac.uk, or by contacting The Cambridge Crystallographic Data Centre, 12 Union Road, Cambridge CB2 1EZ, UK; fax: +44 1223 336033.

AUTHOR INFORMATION

Corresponding Author

*E-mail: m.tamm@tu-bs.de.

ORCID

Matthias Tamm: 0000-0002-5364-0357

Author Contributions

†C.B. and H.E. contributed equally to this work.

Notes

The authors declare no competing financial interest.

ACKNOWLEDGMENTS

We are grateful to the group of Prof. Christophe Copéret (ETH Zurich) for helpful discussions. H.E. thanks the Fonds der Chemischen Industrie (FCI) for a Chemiefonds Fellowship. This work was funded by the Deutsche Forschungsgemeinschaft (DFG) through project TA 189/12–1 (“Mechanistic studies on the catalytic metathesis of internal and terminal alkynes and diyne”).

REFERENCES

- (1) Fürstner, A.; Davies, P. W. *Chem. Commun.* **2005**, 2307–2320.
- (2) Schrock, R. R.; Czekelius, C. *Adv. Synth. Catal.* **2007**, *349*, 55–77.
- (3) Zhang, W.; Moore, J. S. *Adv. Synth. Catal.* **2007**, *349*, 93–120.
- (4) Wu, X.; Tamm, M. *Beilstein J. Org. Chem.* **2011**, *7*, 82–93.
- (5) Jyothish, K.; Zhang, W. *Angew. Chem., Int. Ed.* **2011**, *50*, 8478–8480.
- (6) Fürstner, A. *Angew. Chem., Int. Ed.* **2013**, *52*, 2794–2819.
- (7) Schrock, R. R. *Chem. Commun.* **2013**, *49*, 5529–5531.
- (8) Beer, S.; Hrib, C. G.; Jones, P. G.; Brandhorst, K.; Grunenberg, J.; Tamm, M. *Angew. Chem., Int. Ed.* **2007**, *46*, 8890–8894.
- (9) Beer, S.; Brandhorst, K.; Grunenberg, J.; Hrib, C. G.; Jones, P. G.; Tamm, M. *Org. Lett.* **2008**, *10*, 981–984.
- (10) Beer, S.; Brandhorst, K.; Hrib, C. G.; Wu, X.; Haberlag, B.; Grunenberg, J.; Jones, P. G.; Tamm, M. *Organometallics* **2009**, *28*, 1534–1545.
- (11) Haberlag, B.; Wu, X.; Brandhorst, K.; Grunenberg, J.; Daniliuc, C. G.; Jones, P. G.; Tamm, M. *Chem. - Eur. J.* **2010**, *16*, 8868–8877.
- (12) Lysenko, S.; Daniliuc, C. G.; Jones, P. G.; Tamm, M. *J. Organomet. Chem.* **2013**, *744*, 7–14.
- (13) Haberlag, B.; Freytag, M.; Jones, P. G.; Tamm, M. *Adv. Synth. Catal.* **2014**, *356*, 1255–1265.
- (14) Hötling, S.; Haberlag, B.; Tamm, M.; Collatz, J.; Mack, P.; Steidle, J. L. M.; Vences, M.; Schulz, S. *Chem. - Eur. J.* **2014**, *20*, 3183–3191.
- (15) Ahrens, J.; Haberlag, B.; Scheja, A.; Tamm, M.; Bröring, M. *Chem. - Eur. J.* **2014**, *20*, 2901–2912.
- (16) Buchmeiser, M. R. *Chem. Rev.* **2000**, *100*, 1565–1604.
- (17) Schrock, R. R. *Chem. Rev.* **2002**, *102*, 145–180.
- (18) Schrock, R. R.; Hoveyda, A. H. *Angew. Chem., Int. Ed.* **2003**, *42*, 4592–4633.
- (19) Heppekaussen, J.; Stade, R.; Goddard, R.; Fürstner, A. *J. Am. Chem. Soc.* **2010**, *132*, 11045–11057.
- (20) Heppekaussen, J.; Stade, R.; Kondoh, A.; Seidel, G.; Goddard, R.; Fürstner, A. *Chem. - Eur. J.* **2012**, *18*, 10281–10299.

- (21) Persich, P.; Lloveria, J.; Lhermet, R.; de Haro, T.; Stade, R.; Kondoh, A.; Fürstner, A. *Chem. - Eur. J.* **2013**, *19*, 13047–13058.
- (22) Valot, G.; Mailhol, D.; Regens, C. S.; O'Malley, D. P.; Godineau, E.; Takikawa, H.; Philipps, P.; Fürstner, A. *Chem. - Eur. J.* **2015**, *21*, 2398–2408.
- (23) Willwacher, J.; Heggen, B.; Wirtz, C.; Thiel, W.; Fürstner, A. *Chem. - Eur. J.* **2015**, *21*, 10416–10430.
- (24) Ungeheuer, F.; Fürstner, A. *Chem. - Eur. J.* **2015**, *21*, 11387–11392.
- (25) Cromm, P. M.; Schaubach, S.; Spiegel, J.; Fürstner, A.; Grossmann, T. N.; Waldmann, H. *Nat. Commun.* **2016**, *7*, 11300.
- (26) Cromm, P. M.; Wallraven, K.; Glas, A.; Bier, D.; Fürstner, A.; Ottmann, C.; Grossmann, T. N. *ChemBioChem* **2016**, *17*, 1915–1919.
- (27) Ahlers, A.; de Haro, T.; Gabor, B.; Fürstner, A. *Angew. Chem., Int. Ed.* **2016**, *55*, 1406–1411.
- (28) Schaubach, S.; Michigami, K.; Fürstner, A. *Synthesis* **2016**, *49*, 202–208.
- (29) Lysenko, S.; Haberlag, B.; Daniliuc, C. G.; Jones, P. G.; Tamm, M. *ChemCatChem* **2011**, *3*, 115–118.
- (30) Lysenko, S.; Volbeda, J.; Jones, P. G.; Tamm, M. *Angew. Chem., Int. Ed.* **2012**, *51*, 6757–6761.
- (31) Li, S. T.; Schnabel, T.; Lysenko, S.; Brandhorst, K.; Tamm, M. *Chem. Commun.* **2013**, *49*, 7189–7191.
- (32) Jyothish, K.; Zhang, W. *Angew. Chem., Int. Ed.* **2011**, *50*, 3435–3438.
- (33) Jyothish, K.; Wang, Q.; Zhang, W. *Adv. Synth. Catal.* **2012**, *354*, 2073–2078.
- (34) Yang, H.; Liu, Z.; Zhang, W. *Adv. Synth. Catal.* **2013**, *355*, 885–890.
- (35) Du, Y.; Yang, H.; Zhu, C.; Ortiz, M.; Okochi, K. D.; Shoemaker, R.; Jin, Y.; Zhang, W. *Chem. - Eur. J.* **2016**, *22*, 7959–7963.
- (36) Zhu, Y.; Yang, H.; Jin, Y.; Zhang, W. *Chem. Mater.* **2013**, *25*, 3718–3723.
- (37) Paley, D. W.; Sedbrook, D. F.; Decatur, J.; Fischer, F. R.; Steigerwald, M. L.; Nuckolls, C. *Angew. Chem., Int. Ed.* **2013**, *52*, 4591–4594.
- (38) Yang, H.; Jin, Y.; Du, Y.; Zhang, W. *J. Mater. Chem. A* **2014**, *2*, 5986.
- (39) Lu, G.; Yang, H.; Zhu, Y.; Huggins, T.; Ren, Z. J.; Liu, Z.; Zhang, W. *J. Mater. Chem. A* **2015**, *3*, 4954–4959.
- (40) Zhang, C.; Wang, Q.; Long, H.; Zhang, W. *J. Am. Chem. Soc.* **2011**, *133*, 20995–21001.
- (41) Zhang, C.; Long, H.; Zhang, W. *Chem. Commun.* **2012**, *48*, 6172–6174.
- (42) Yu, C.; Long, H.; Jin, Y.; Zhang, W. *Org. Lett.* **2016**, *18*, 2946–2949.
- (43) Wang, Q.; Zhang, C.; Noll, B. C.; Long, H.; Jin, Y.; Zhang, W. *Angew. Chem., Int. Ed.* **2014**, *53*, 10663–10667.
- (44) Wang, Q.; Yu, C.; Long, H.; Du, Y.; Jin, Y.; Zhang, W. *Angew. Chem., Int. Ed.* **2015**, *54*, 7550–7554.
- (45) Wang, Q.; Yu, C.; Zhang, C.; Long, H.; Azarnoush, S.; Jin, Y.; Zhang, W. *Chem. Sci.* **2016**, *7*, 3370–3376.
- (46) Ortiz, M.; Cho, S.; Niklas, J.; Kim, S.; Poluektov, O. G.; Zhang, W.; Rumbles, G.; Park, J. *J. Am. Chem. Soc.* **2017**, *139*, 4286–4289.
- (47) Schrock, R. R. *Polyhedron* **1995**, *14*, 3177–3195.
- (48) Buhro, W. E.; Chisholm, M. H. *Adv. Organomet. Chem.* **1987**, *27*, 311–369.
- (49) Schrock, R. R.; Clark, D. N.; Sancho, J.; Wengrovius, J. H.; Rocklage, S. M.; Pedersen, S. F. *Organometallics* **1982**, *1*, 1645–1651.
- (50) Freudenberger, J. H.; Schrock, R. R.; Churchill, M. R.; Rheingold, A. L.; Ziller, J. W. *Organometallics* **1984**, *3*, 1563–1573.
- (51) McCullough, L. G.; Schrock, R. R. *J. Am. Chem. Soc.* **1984**, *106*, 4067–4068.
- (52) McCullough, L. G.; Schrock, R. R.; Dewan, J. C.; Murdzek, J. C. *J. Am. Chem. Soc.* **1985**, *107*, 5987–5998.
- (53) Wengrovius, J. H.; Sancho, J.; Schrock, R. R. *J. Am. Chem. Soc.* **1981**, *103*, 3932–3934.
- (54) Haberlag, B.; Freytag, M.; Daniliuc, C. G.; Jones, P. G.; Tamm, M. *Angew. Chem., Int. Ed.* **2012**, *51*, 13019–13022.

- (55) Estes, D. P.; Bittner, C.; Àrias, Ò.; Casey, M.; Fedorov, A.; Tamm, M.; Copéret, C. *Angew. Chem., Int. Ed.* **2016**, *55*, 13960–13964.
- (56) Hötling, S.; Bittner, C.; Tamm, M.; Dähn, S.; Collatz, J.; Steidle, J. L. M.; Schulz, S. *Org. Lett.* **2015**, *17*, 5004–5007.
- (57) Lhermet, R.; Fürstner, A. *Chem. - Eur. J.* **2014**, *20*, 13188–13193.
- (58) Bray, A.; Mortreux, A.; Petit, F.; Petit, M.; Szymanska-Buzar, T. *J. Chem. Soc., Chem. Commun.* **1993**, 197–199.
- (59) Mortreux, A.; Petit, F.; Petit, M.; Szymanska-Buzar, T. *J. Mol. Catal. A: Chem.* **1995**, *96*, 95–105.
- (60) Coutelier, O.; Mortreux, A. *Adv. Synth. Catal.* **2006**, *348*, 2038–2042.
- (61) Coutelier, O.; Nowogrocki, G.; Paul, J.-F.; Mortreux, A. *Adv. Synth. Catal.* **2007**, *349*, 2259–2263.
- (62) McCullough, L. G.; Listemann, M. L.; Schrock, R. R.; Churchill, M. R.; Ziller, J. W. *J. Am. Chem. Soc.* **1983**, *105*, 6729–6730.
- (63) Freudenberger, J. H.; Schrock, R. R. *Organometallics* **1986**, *5*, 1411–1417.
- (64) von Kugelgen, S.; Bellone, D. E.; Cloke, R. R.; Perkins, W. S.; Fischer, F. R. F. *J. Am. Chem. Soc.* **2016**, *138*, 6234–6239.
- (65) von Kugelgen, S.; Sifri, R.; Bellone, D.; Fischer, F. R. F. *J. Am. Chem. Soc.* **2017**, *139*, 7577–7585.
- (66) Gilbert, T. M.; Landes, A. M.; Rogers, R. D. *Inorg. Chem.* **1992**, *31*, 3438–3444.
- (67) Becke, A. D. *J. Chem. Phys.* **1993**, *98*, 5648–5652.
- (68) Stephens, P. J.; Devlin, F. J.; Chabalowski, C. F.; Frisch, M. J. *J. Phys. Chem.* **1994**, *98*, 11623–11627.
- (69) Zhu, J.; Jia, G.; Lin, Z. *Organometallics* **2006**, *25*, 1812–1819.
- (70) Frisch, M. J.; Trucks, G. W.; Schlegel, H. B.; Scuseria, G. E.; Robb, M. A.; Cheeseman, J. R.; Scalmani, G.; Barone, V.; Petersson, G. A.; Nakatsujii, H.; Li, X.; Caricato, M.; Marenich, A.; Bloino, J.; Janesko, B. G.; Gomperts, R.; Mennucci, B.; Hratchian, H. P.; Ortiz, J. V.; Izmaylov, A. F.; Sonnenberg, J. L.; Williams-Young, D.; Ding, F.; Lipparini, F.; Egidi, F.; Goings, J.; Peng, F.; Petrone, A.; Henderson, T.; Ranasinghe, D.; Zakrzewski, V. G.; Gao, J.; Rega, N.; Zheng, G.; Liang, W.; Hada, M.; Ehara, M.; Toyota, K.; Fukuda, R.; Hasegawa, J.; Ishida, M.; Nakajima, T.; Honda, Y.; Kitao, O.; Nakai, H.; Vreven, T.; Throssell, K.; Montgomery, J. A.; Peralta, J. E., JR.; Ogliaro, F.; Bearpark, M.; Heyd, J. J.; Brothers, E.; Kudin, K. N.; Staroverov, V. N.; Keith, T.; Kobayashi, R.; Normand, J.; Raghavachari, K.; Rendell, A.; Burant, J. C.; Iyengar, S. S.; Tomasi, J.; Cossi, M.; Millam, J. M.; Klene, M.; Adamo, A.; Cammi, R.; Ochterski, J. W.; Martin, R. L.; Morokuma, K.; Farkas, O.; Foresman, J. B.; Fox, D. J. *Gaussian 09*, revision D.01; Gaussian, Inc.: Wallingford, CT, 2016.
- (71) Vyboishchikov, S. F.; Bühl, M.; Thiel, W. *Chem. - Eur. J.* **2002**, *8*, 3962–3975.
- (72) Katz, T. J.; McGinnis, J. *J. Am. Chem. Soc.* **1975**, *97*, 1592–1594.
- (73) Suresh, C. H.; Frenking, G. *Organometallics* **2012**, *31*, 7171–7180.
- (74) Woo, T.; Folga, E.; Ziegler, T. *Organometallics* **1993**, *12*, 1289–1298.
- (75) Remya, P. R.; Suresh, C. H. *Dalton Trans.* **2016**, *45*, 1769–1778.
- (76) Fürstner, A.; de Souza, D.; Turet, L.; Fenster, M. D. B.; Parra-Rapado, L.; Wirtz, C.; Mynott, R.; Lehmann, C. W. *Chem. - Eur. J.* **2007**, *13*, 115–134.
- (77) Fürstner, A.; Guth, O.; Rumbo, A.; Seidel, G. *J. Am. Chem. Soc.* **1999**, *121*, 11108–11113.
- (78) Fürstner, A.; Seidel, G. *Angew. Chem., Int. Ed.* **1998**, *37*, 1734–1736.
- (79) Listemann, M. L.; Schrock, R. R. *Organometallics* **1985**, *4*, 74–83.
- (80) Schrock, R. R.; Jamieson, J. Y.; Araujo, J. P.; Bonitatebus, P. J.; Sinha, A.; Lopez, L. H. *J. Organomet. Chem.* **2003**, *684*, 56–67.
- (81) Pedersen, S. F.; Schrock, R. R.; Churchill, M. R.; Wasserman, H. *J. Am. Chem. Soc.* **1982**, *104*, 6808–6809.
- (82) Churchill, M. R.; Ziller, J. W.; Freudenberger, J. H.; Schrock, R. R. *Organometallics* **1984**, *3*, 1554–1562.
- (83) O'Reilly, M. E.; Ghiviriga, I.; Abboud, K. A.; Veige, A. S. *Dalton Trans.* **2013**, *42*, 3326–3336.
- (84) Àrias, Ò.; Brandhorst, K.; Baabe, D.; Freytag, M.; Jones, P. G.; Tamm, M. *Dalton Trans.* **2017**, *46*, 4737–4748.